

Studies of e^+e^- Collisions with a Hard Initial-State Photon at BaBar *

Nicolas Berger

Representing the BaBar Collaboration
SLAC MS 61, Menlo Park, California, U.S.A.

We present preliminary BaBar measurements of hadronic cross sections in e^+e^- annihilation using the radiative return technique. The cross sections for $e^+e^- \rightarrow p\bar{p}$, $3(\pi^+\pi^-)$, $2(\pi^+\pi^-)2\pi^0$, and $K^+K^-2(\pi^+\pi^-)$ are measured. Measurements of the proton form factor and of the ratio G_E/G_M are also shown.

I. INTRODUCTION

In recent years, precise new results in low-energy hadronic cross sections have been obtained at high-luminosity e^+e^- machines using the radiative return technique. The cross section for $e^+e^- \rightarrow \pi^+\pi^-$ has been measured by the KLOE collaboration [1], while those of $e^+e^- \rightarrow \pi^+\pi^-\pi^0$, $\pi^+\pi^-\pi^+\pi^-$, $K^+K^-K^+K^-$ and $K^+K^-\pi^+\pi^-$ have been measured by BaBar [2, 3]. These measurements are of particular interest since they provide input to data-driven calculations of hadronic contributions to the muon anomalous magnetic moment, a_μ^{had} , and of the running of the QED coupling constant $\Delta\alpha_{had}^{(5)}$, which appears in global fits to the standard model. As a continuation of this program, preliminary BaBar measurements for the $p\bar{p}$, $3(\pi^+\pi^-)$, $2(\pi^+\pi^-)2\pi^0$, and $K^+K^-2(\pi^+\pi^-)$ final states are presented here. The $p\bar{p}$ and six-hadron results are based on 240 fb^{-1} and 232 fb^{-1} of data respectively.

II. RADIATIVE RETURN

The radiative return method uses the emission of an initial-state photon to probe center-of-mass energies $\sqrt{s'}$ below the nominal collision energy \sqrt{s} . The emission of a photon of energy E_γ in the center-of-mass frame corresponds to the production of a recoiling system with $s' = s - 2\sqrt{s}E_\gamma$. Cross-section measurements can therefore be obtained over a wide range of center-of-mass energies without varying the beam energy, thereby avoiding the usual point-to-point uncertainties associated with discrete measurements.

At BaBar the range $\sqrt{s'} \leq 4.5\text{ GeV}$ is readily accessible. To reduce backgrounds, events are reconstructed by requiring the ISR photon to be detected within the acceptance of the BaBar electromagnetic calorimeter. Since the recoiling system is produced as a jet opposite the high-energy photon, the event detection efficiency is only weakly dependent on $\sqrt{s'}$, and measurements down to threshold are possible. The efficiency also does not depend strongly on the simulation of the hadronic final state.

At first order the cross section for an ISR process with a photon polar angle acceptance of $\theta_{min} < \theta_\gamma < \pi - \theta_{min}$ in the center-of-mass frame is

$$\frac{d\sigma_{e^+e^- \rightarrow \gamma X}}{dx} = \frac{\alpha}{\pi} \frac{1+x^2}{x(1-x)} \left(\log \frac{1 - \cos\theta_{min}}{1 + \cos\theta_{min}} - (1-x)\cos\theta_{min} \right) \sigma_{e^+e^- \rightarrow X}(s(1-x)) \quad (1)$$

where $x = 1 - s'/s$. A kinematic fit is used to measure s' and reject backgrounds. Cross sections are normalized using the process $e^+e^- \rightarrow \mu^+\mu^-\gamma$.

III. THE $p\bar{p}$ FINAL STATE

The cross section for $e^+e^- \rightarrow p\bar{p}$ is given by

* Work supported by Department of Energy contract DE-AC02-76SF00515.

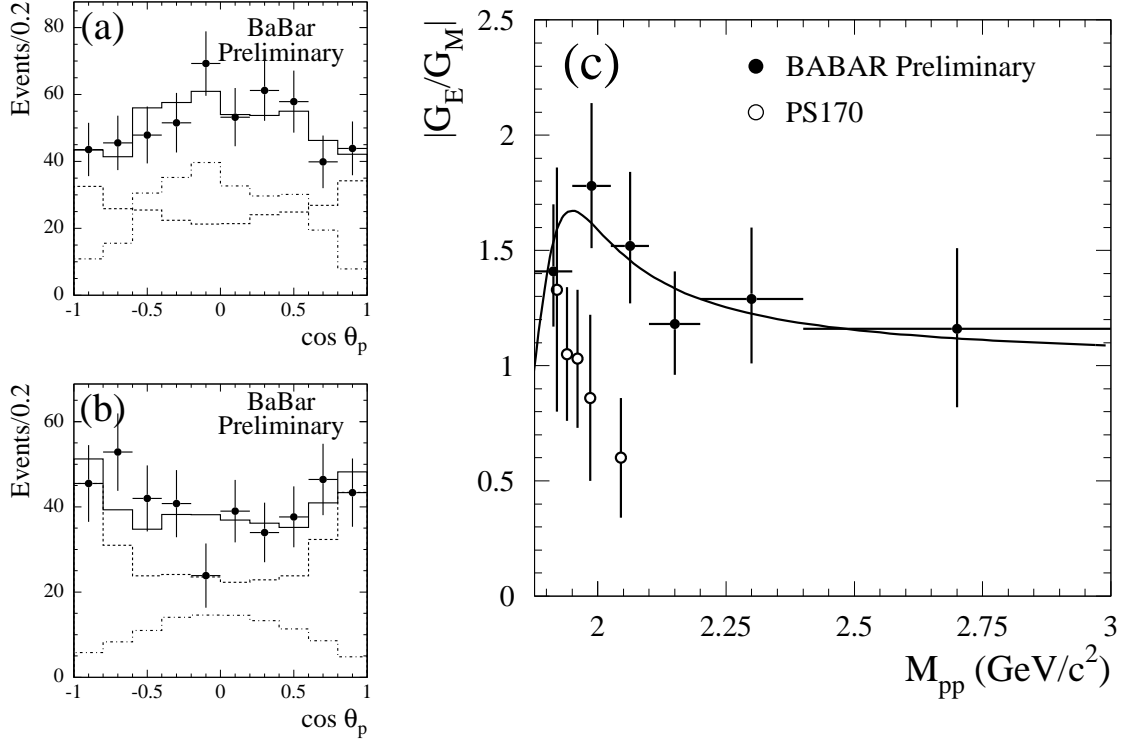


FIG. 1: $\cos \theta_p$ distributions for the mass bins $[1.877; 1.950] \text{ GeV}/c^2$ (a) and $[2.400; 3.000] \text{ GeV}/c^2$ (b). The dashed (dot-dashed) curve shows the contribution from the simulated $|G_M|^2$ ($|G_E|^2$) cross section term; the solid line is the sum of the two terms and the points correspond to data. (c) Mass dependence of the ratio $|G_E/G_M|$.

$$\sigma_{e^+e^- \rightarrow p\bar{p}}(s') = \frac{4\pi\alpha^2 C}{3s'} \sqrt{1 - \frac{2m_p^2}{s'}} \left(|G_M(s')|^2 + \frac{2m_p^2}{s'} |G_E(s')|^2 \right), \quad (2)$$

where m_p is the proton mass and G_E and G_M are respectively the electric and magnetic form factors of the proton. The factor C accounts for Coulomb interaction in the $p\bar{p}$ system and has the effect of making the cross section non-zero at threshold.

The detection efficiency for the ISR process is about 17%, with no strong dependence on either the $p\bar{p}$ invariant mass $m_{p\bar{p}}$ or the value of $|G_E/G_M|$.

The proton helicity angle θ_p in the $p\bar{p}$ rest frame can be used to separate the $|G_E|^2$ and $|G_M|^2$ terms. Their respective variations are approximately $\sin^2 \theta_p$ and $1 + \cos^2 \theta_p$, with exact expressions obtained from Monte-Carlo simulation. By fitting the $\cos \theta_p$ distribution to a sum of the two terms the ratio $|G_E/G_M|$ can be extracted. This is done separately in six bins of $m_{p\bar{p}}$. Preliminary results are shown in Fig. 1, and disagree significantly with previous measurements from LEAR [7].

The cross section for $e^+e^- \rightarrow p\bar{p}$ is measured and from it we obtain the “effective form factor” $G = \sqrt{|G_E|^2 + 2m_p^2/s'|G_M|^2}$. Preliminary values are shown in Figs. 2(a) and 2(b). Results are in good agreement with existing data, and cover the entire energy range from threshold to 4.5 GeV in a single measurement. The data show a clear enhancement at threshold, already observed by LEAR, as well as hints of structures at 2.25 and 3 GeV/ c^2 . Apart from these structures, the data agree well with a fit to the perturbative QCD expectation [4, 5] $G(m_{p\bar{p}}) = A/m_{p\bar{p}}^4 \log(m_{p\bar{p}}^2/\Lambda^2)$, where A and Λ are constants determined from the fit, which is shown as the dashed curve in Fig. 2(a).

IV. FINAL STATES WITH SIX HADRONS

As an extension of the recent ISR measurements of the cross section of final states with four pions or kaons [3], preliminary results have been obtained for the six-hadron processes $e^+e^- \rightarrow 3(\pi^+\pi^-)$, $2(\pi^+\pi^-)2\pi^0$ and $K^+K^-2(\pi^+\pi^-)$.

Mode	Branching fraction (this work)	Branching Fraction (PDG)
$J/\psi \rightarrow 3(\pi^+\pi^-)$	$(4.40 \pm 0.29 \pm 0.29) \times 10^{-3}$	$(4.0 \pm 2.0) \times 10^{-3}$
$J/\psi \rightarrow 2(\pi^+\pi^-)2\pi^0$	$(1.65 \pm 0.10 \pm 0.18) \times 10^{-2}$	n/a
$J/\psi \rightarrow K^+K^-2(\pi^+\pi^-)$	$(5.09 \pm 0.42 \pm 0.35) \times 10^{-3}$	$(3.1 \pm 1.3) \times 10^{-3}$
$\psi(2S) \rightarrow 2(\pi^+\pi^-)2\pi^0$	$(5.3 \pm 1.6 \pm 0.6) \times 10^{-3}$	n/a
$\psi(2S) \rightarrow K^+K^-2(\pi^+\pi^-)$	$(2.1 \pm 1.0 \pm 0.2) \times 10^{-3}$	n/a

TABLE I: Summary of J/ψ and $\psi(2S)$ branching fraction obtained from six-hadron final states

The corresponding cross section distributions are shown in Figs. 2(c), 2(d) and 2(e) respectively. In the $2(\pi^+\pi^-)2\pi^0$ mode the data disagree strongly with the DM2 results above 1.8 GeV. Apart from this, the data agrees well with existing results, and is considerably more precise. The cross section for $K^+K^-2(\pi^+\pi^-)$ is measured for the first time. Again, the entire energy range from threshold to 4.5 GeV is covered in a single experiment.

A clear dip is visible at about 1.9 GeV in the 6π modes. A similar feature was already seen by DM2 in $e^+e^- \rightarrow 3(\pi^+\pi^-)$ and by FOCUS [8] in the diffractive photoproduction of six charged pions. The cross section distributions are fitted using the parametrization used by FOCUS, a sum of a Breit-Wigner resonance shape and a Jacob-Slansky continuum [6]. For the $3(\pi^+\pi^-)$ ($2(\pi^+\pi^-)2\pi^0$) mode, we obtain values of 1880 ± 30 MeV (1860 ± 20 MeV) for the resonance peak, 130 ± 30 MeV (160 ± 20 MeV) for the resonance width and 21 ± 14 deg (-3 ± 15 deg) for phase shift between the resonance and continuum. The width values differ significantly from the FOCUS result of 29 ± 14 MeV.

In the $3(\pi^+\pi^-)$ channel the resonance structure is surprisingly simple, being well-described by a Monte-Carlo simulation featuring a single $\rho^0 \rightarrow \pi^+\pi^-$ resonance and the other four pions distributed according to phase space. However rich resonant structures are observed in the $2(\pi^+\pi^-)2\pi^0$ channel, with signals for $\rho^0 \rightarrow \pi^+\pi^-$, $\rho^+ \rightarrow \pi^+\pi^0$, $f_0 \rightarrow \pi^0\pi^0$ and $f_0(1270) \rightarrow \pi^+\pi^-$ in the 2π combinations, and signals for ω and η in $\pi^+\pi^-\pi^0$. A signal for $e^+e^- \rightarrow \omega(\pi^+\pi^-\pi^0)\eta(\pi^+\pi^-\pi^0)$ is also seen, corresponding to a resonant structure in the 6π invariant mass, as shown in Fig. 2(f). Fitting the distribution to a Breit-Wigner shape gives a peak position of 1645 ± 8 MeV and a width of 114 ± 14 MeV, which could correspond to the ω'' state reported in our previous analysis of the $\pi^+\pi^-\pi^0$ final state [2]. Apart from this structure, which is unique to the $2(\pi^+\pi^-)2\pi^0$ mode, the ratio of the $2(\pi^+\pi^-)2\pi^0$ and $3(\pi^+\pi^-)$ cross sections is remarkably constant over the entire energy range, at a value of $3.98 \pm 0.06(\text{stat.}) \pm 0.41(\text{syst.})$. In the $K^+K^-2(\pi^+\pi^-)$ final state, a signal for $\phi \rightarrow K^+K^-$ is seen, with a significant contribution from $J/\psi \rightarrow \phi\pi^+\pi^-\pi^+\pi^-$. Signals for $K^{*0} \rightarrow K^+\pi^-$ are also present. Finally, the observed J/ψ and $\psi(2S)$ signals can be used to extract branching fraction measurements which, in many cases, considerably improve over current world averages. These results are summarized in Table I.

V. CONCLUSION

The program to measure low-energy hadronic cross sections using ISR is well underway at BaBar. In addition to the published results for $\pi^+\pi^-\pi^0$, $2(\pi^+\pi^-)$, $K^+K^-\pi^+\pi^-$ and $2(K^+K^-)$, we now have preliminary results for the $3(\pi^+\pi^-)$, $2(\pi^+\pi^-)2\pi^0$, $K^+K^-2(\pi^+\pi^-)$ and $p\bar{p}$ modes, with analyses ongoing for the final states $\pi^+\pi^-$, K^+K^- , $\pi^+\pi^-\pi^0\pi^0$, η , η' , and $D^{(*)}\bar{D}^{(*)}$.

VI. ACKNOWLEDGMENTS

The author is grateful for the extraordinary contributions of the PEP-II colleagues in achieving the excellent luminosity and machine conditions that have made this work possible. This work is supported by DOE and NSF (USA), NSERC (Canada), IHEP (China), CEA and CNRS-IN2P3 (France), BMBF and DFG (Germany), INFN (Italy), FOM (The Netherlands), NFR (Norway), MIST (Russia), and PPARC (United Kingdom). Individuals have received support from CONACyT (Mexico), A. P. Sloan Foundation, Research Corporation, and Alexander von Humboldt Foundation.

-
- [1] S.E. Muller *et al.*, Nucl. Phys. Proc. Suppl. **126**, 335-340 (2004)
 - [2] B. Aubert *et al.*, Phys. Rev. D **70**, 072004 (2004)
 - [3] B. Aubert *et al.*, Phys. Rev. D **71**, 052001 (2005)

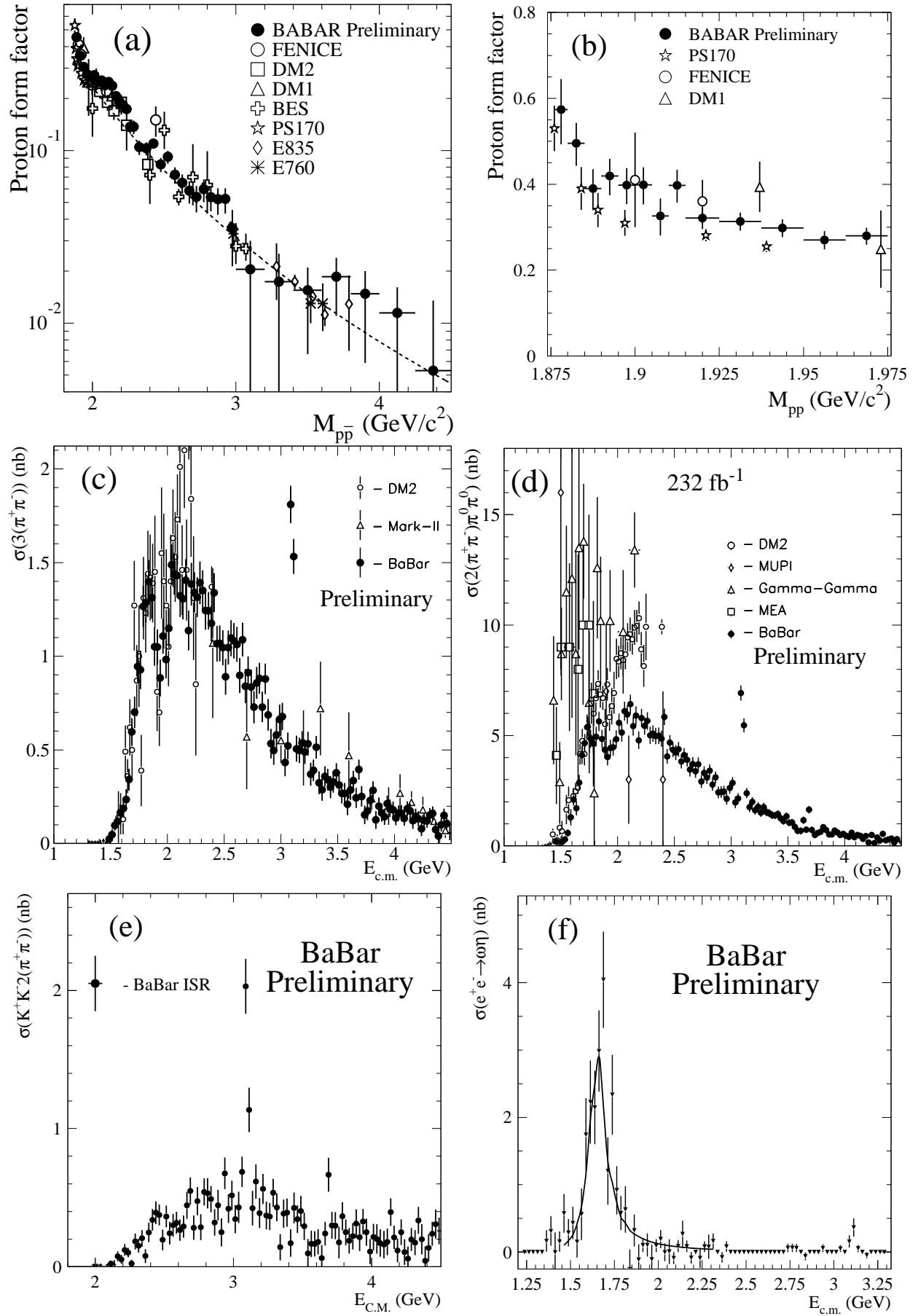


FIG. 2: (a) Effective proton form factor versus $m_{p\bar{p}}$; (b) Close-up view of the threshold region. Cross section distributions versus \sqrt{s} invariant mass for (c) $e^+e^- \rightarrow 3(\pi^+\pi^-)$, (d) $2(\pi^+\pi^-)2\pi^0$, (e) $K^+K^-2(\pi^+\pi^-)$, and (f) $e^+e^- \rightarrow \omega(\pi^+\pi^-\pi^0)\eta(\pi^+\pi^-\pi^0)$.

- [4] V. L. Chernyak and A. R. Zhitinsky, JETP Lett. **25**, 510 (1977)
- [5] P. Lepage and S. Brodsky, Phys. Rev. Lett **43**, 545 (1979)
- [6] M. Jacob and R. Slansky, Phys. Rev. Lett **B37**, 408 (1971) and Phys. Rev. D **5**, 1847 (1972)
- [7] G. Bardin *et al.*, Nucl. Phys. B **411**, 3 (1994)
- [8] E687 Collaboration: P.L. Frabetti *et al.*, Phys. Lett. **B514**, 240-246 (2001)